ACS APPLIED MATERIALS & INTERFACES

Research Article

www.acsami.org

TiO_2/ZnO Inner/Outer Double-Layer Hollow Fibers for Improved Detection of Reducing Gases

Akash Katoch, Jae-Hun Kim, and Sang Sub Kim*

Department of Materials Science and Engineering, Inha University, Incheon 402-751, Republic of Korea

Supporting Information

ABSTRACT: TiO_2/ZnO double-layer hollow fibers (DLHFs) are proposed as a superior sensor material in comparison to regular single-layer hollow fibers (HFs) for the detection of reducing gases. DLHFs were synthesized on sacrificial polymer fibers via atomic layer deposition of a first layer of TiO_2 followed by a second layer of ZnO and by a final thermal treatment. The inner TiO_2 receives electrons from the ZnO outer layer, which becomes more resistive due to the significant loss of electrons. This highly resistive ZnO layer partially regains its original resistivity when exposed to reducing gases such as CO, thus enabling more resistance variation in DLHFs. DLHFs are a novel material compared to HFs and can be successfully employed to fabricate chemical sensors for the accurate detection of reducing gases.

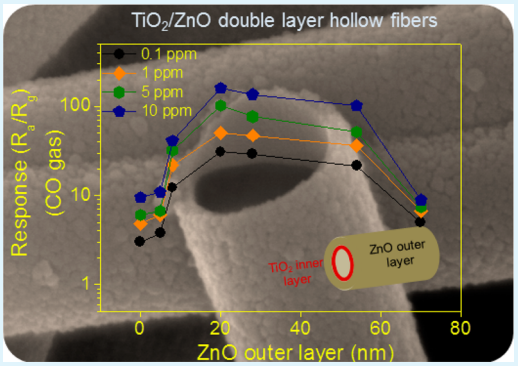

KEYWORDS: *electrospinning, hollow fiber, double layer, TiO_2, ZnO, gas sensor, Debye length*

1. INTRODUCTION

Oxide fibers usually synthesized by electrospinning have been widely investigated for their potential applications in fields where reactions taking place on the surface are of high importance, including sensors, filters and catalysis. This is due to their advantageous attributes, including a wide range of potentially achievable diverse morphologies, a large surface area, their high reproducibility, and the relatively low cost of production.[1,2] In particular, oxide fibers are considered a promising material in the production of sensors for detection of gaseous chemical species.[3] The key parameters affecting the sensing capabilities of oxide fibers have been largely investigated and identified.[4]

For instance, one of the routes adopted to improve the sensing properties of oxide fibers is tailoring their morphology. Hollow fibers (HFs) have emerged as a better material for gas sensing applications than regular solid fibers.[5−9] The available surface area is significantly increased by the cavity running along the whole length of the fiber and providing both an outer and an inner surface, thus conferring HFs a superior sensing performance compared to regular solid fibers.

A further route followed to improve HFs' sensing properties is the optimization of the fiber wall thickness. The ideal behavior is expected when the wall thickness is thinner than the space charge layer established at the interface with the reducing gas and equivalent to the Debye length, λ_D, of the HF's material. Accordingly, when the whole fiber wall in a HF is completely depleted of electrons, the resistance variation under exposure to reducing gases will reach a maximum.

In general, the typical λ_D of oxide materials corresponds to a few tens of nanometers. For instance, λ_D of ZnO varies in the range of 20−35 nm depending on the temperature and carrier concentration.[10,11] This means that the commonly prepared ZnO HFs reach the best sensing properties for reducing gases when their wall thickness is thinner than 20−35 nm. Such a thin wall is quite challenging to achieve because of the risk of collapse of HFs during the stage immediately following the thermal treatment used to remove the sacrificial polymer fibers.

In the present study, we propose a novel methodology to fabricate regular HFs, where the fiber wall is completely electron-depleted even when thicker than λ_D. This is achieved by employing a double-layer oxide system, namely TiO_2/ZnO double-layer hollow fibers (DLHFs). Here, an electron flow takes place from the outer ZnO layer to the inner Ti_2O one. When the TiO_2 inner layer receives electrons from the ZnO outer layer, complete electron depletion in the ZnO layer is promoted, thus overcoming the limitations related to the ideal ratio between the fiber wall thickness and the λ_D.

2. EXPERIMENTAL SECTION

Synthesis of TiO_2/ZnO DLHFs. TiO_2/ZnO DLHFs were synthesized by using a three-step process. First, polyvinyl acetate (PVA, M_w = 80 000, Sigma-Aldrich) fibers were synthesized by electrospinning; subsequently, TiO_2 and ZnO layers were sequentially deposited on the PVA fibers by atomic layer deposition (ALD) and, finally, a thermal treatment was performed for the removal of the PVA fibers used as a sacrificial template, in order to achieve a hollow structure. For TiO_2 deposition, H_2O and titanium(IV) isopropoxide ($Ti(OCH(CH_3)_2)_4$, TTIP) were used as precursors. H_2O and TTIP

Received: September 22, 2014
Accepted: November 7, 2014
Published: November 7, 2014

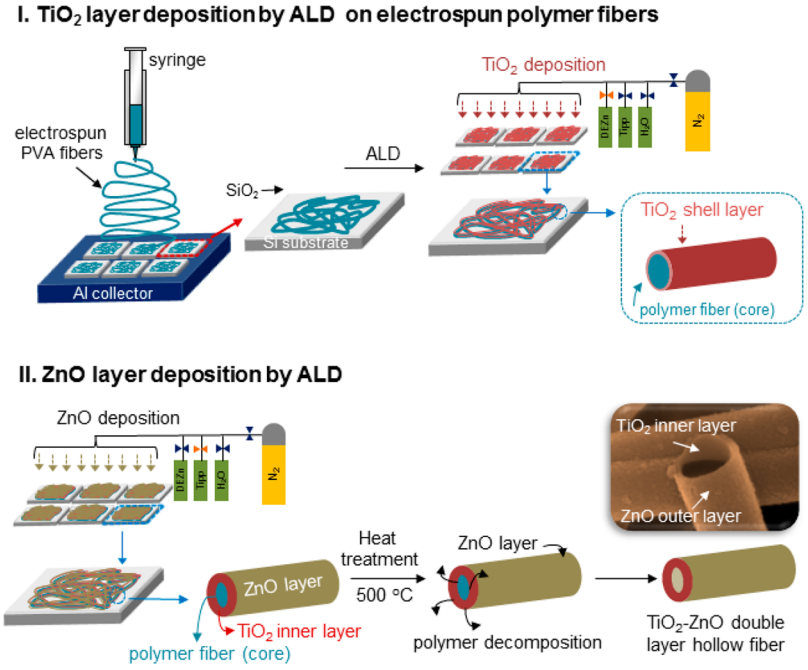

Figure 1. Schematic diagram of the TiO_2/ZnO DLHFs fabrication process.

were separately introduced into the growth reactor to prevent a vigorous prereaction of the two precursors while keeping the temperature and pressure in the reactor at 150 °C and 0.1 torr, respectively. H_2O and TTIP were kept in bubblers at 25° and 40 °C, respectively. The typical ALD pulse lengths were set at 1 s for TTIP dosing, 10 s for N_2 purging, 0.2 s for H_2O dosing, and 25 s for N_2 purging. The ALD cycle was repeated 1000 times, producing a 30 nm-thick oxide layer on the core PVA fibers. For ZnO deposition, diethylzinc ($Zn(C_2H_5)_2$, DEZn) and H_2O were used as precursors. During deposition, the temperature and pressure of the ALD reactor were maintained at 150 °C and 0.3 torr, respectively. The ALD pulse length was set to 0.12 s for dosing of DEZn, 3 s for purging with N_2, 0.15 s for dosing of H_2O, and 3 s for purging with N_2. The thickness of the ZnO layer was in the range 3−70 nm and was achieved by repeating the ALD cycle between 20 and 350 times. The experimental procedure for the deposition of TiO_2 and ZnO layers using ALD is described in detail in the earlier reports of our research group.[7,12] The thermal treatment was performed by baking the achieved TiO_2/ZnO/PVA fibers at 500 °C for 30 min until the core PVA fibers were completely removed. Schematic diagrams detailing the procedure for the synthesis of DLHFs are shown in Figure 1.

Microstructure Observation. The microstructure of DLHFs was investigated by field-emission scanning electron microscopy (FE-SEM) and transmission electron microscopy (TEM), whereas the crystalline phases were studied using X-ray diffraction (XRD) analysis. Energy dispersive spectroscopy (EDS) analysis was carried out to identify their chemical composition.

Sensing Measurement. For the sensing measurements, a titanium/gold electrode (~50 nm Ti/ ~200 nm Au) was deposited on the synthesized DLHFs via sequential sputtering of titanium and gold targets. A metallic mask placed on the surface of the DLHFs allowed obtaining interdigitated comb-shaped electrodes. The performances of the fabricated sensors were investigated under exposure to CO and NO_2 as representative of a reducing and an oxidizing gas, respectively. Measurements were performed at a temperature 375 °C, chosen on the basis of preliminary experiments,[13] using a gas sensing system. Details of the sensing system and measurement process are given in the earlier reports of our research group.[2,14] The response under gas exposure was determined according to the equation:

$$\text{response} = R_a/R_g \quad (1)$$

for CO, and according to the equation:

$$\text{response} = R_g/R_a \quad (2)$$

for NO_2, where R_a and R_g are the resistance in the absence and in the presence of the target gas, respectively.

3. RESULTS AND DISCUSSION

Representative FE-SEM images showing the microstructure of TiO_2/ZnO DLHFs with varying ZnO layer thickness are reported in Figure 2a−f. Insets show the corresponding low-magnification images, revealing the overall morphology of the DLHFs. For comparison, the microstructure of regular, single-layer TiO_2 HFs is shown in Figure 2a. The average fiber wall thickness and inner diameter of TiO_2 HFs were ~30 and ~320 nm, respectively. Note that their surface appears relatively smooth, with no apparent grains. On these TiO_2 HFs, ZnO layers were subsequently deposited, producing TiO_2/ZnO DLHFs. It is evident that the surface of the outer ZnO layers becomes rougher as their thickness increases. The microstructure of DLHFs with an 8 nm thick ZnO layer was further investigated by TEM, and the results are shown in Figure 2g−i. As evident in Figure 2g, the presence of a dark border and a semitransparent core region confirms the hollow nature of DLHFs. The outer ZnO layer covers uniformly the surface of the inner TiO_2 layer, despite its very low thickness. Figure 2h is a high-magnification TEM image from a region of the ZnO layer where the lattice fringe matches well with the distance between the (101) planes of ZnO (0.25 nm). The line profiles for Zn (blue), Ti (red), and O (black) are shown in Figure 2i, confirming again the hollow nature of TiO_2/ZnO DLHFs. The XRD patterns, as shown in Figure S1 of the Supporting Information, reveal the tetragonal structure of pure anatase for the TiO_2 layer (JCPDS Card No. 89-4921) and the hexagonal structure for the ZnO layer (JCPDS Card No. 89-0511). The increase in peak intensity of the ZnO phase mirrors the increase in ZnO layer thickness. Both the microstructure and crystalline structure investigation consistently demonstrate the successful synthesis of TiO_2/ZnO DLHFs.

dx.doi.org/10.1021/am506499e | ACS Appl. Mater. Interfaces 2014, 6, 21494−21499

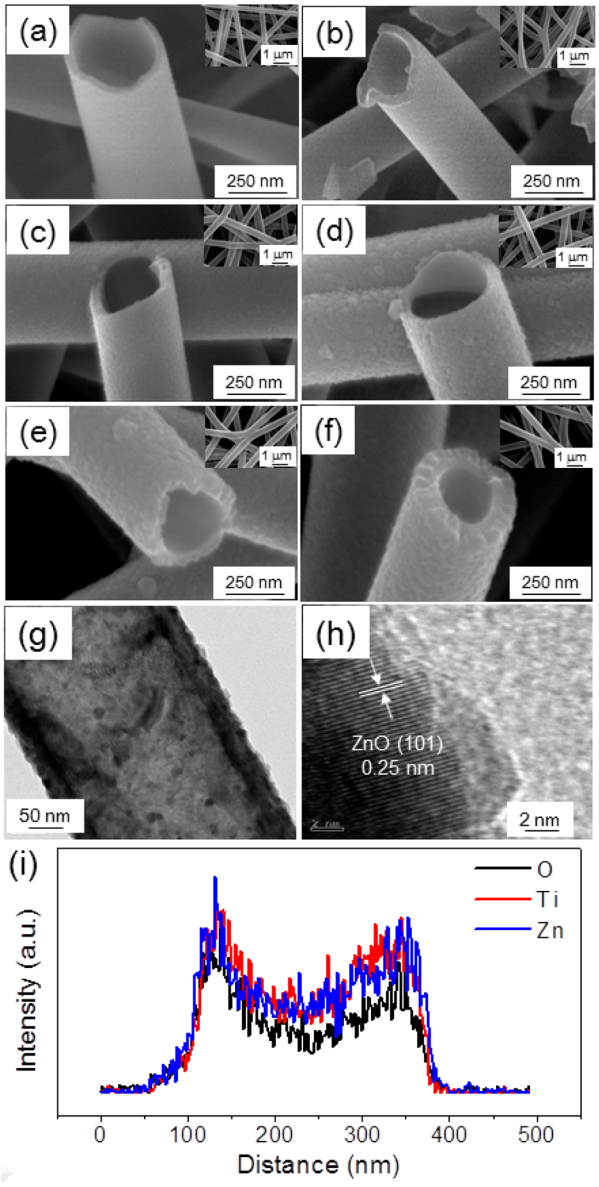

Figure 2. Typical FE-SEM images of (a) TiO_2 HFs prepared with 1000 ALD cycles; TiO_2/ZnO DLHFs prepared with (b) 20 ALD cycles, (c) 50 ALD cycles, (d) 90 ALD cycles, (e) 220 ALD cycles, and (f) 350 ALD cycles. (g) TEM image of a TiO_2/ZnO DLHF with 8 nm thick ZnO outer layer and (h) high magnification image of the ZnO outer layer. (i) EDS line profiles along the fiber radial direction.

The sensing performances of DLHFs with varying thickness of ZnO were investigated under exposure to CO and NO_2. The dynamic resistance curves of DLHFs relative to varying concentrations of CO are shown in Figure S2 of the Supporting Information. The results relative to TiO_2 HFs are included for comparison. The sensor response is evidently influenced by the ZnO layer thickness. The results relative to the sensing performances of DLHFs under exposure to NO_2 are shown in Figure S3 of the Supporting Information. The resistance of DLHFs increases when exposed to NO_2 and decreases when exposure is terminated, a characteristic behavior of *n*-type semiconductors. It is of note that some dynamic resistance curves of DLHFs were not horizontal, showing nonsaturated behavior. This is likely to come from the sluggish desorption kinetics of gas molecules on semiconductor surface. However, the degree of nonsaturation is very small, indicating that the resistance values taken from the curves were valid.

Figure 3 summarizes the DLHFs responses to CO and NO_2. The response curve of 52 nm-thick single-layer ZnO HFs is included for comparison. The resistance of DLHFs-based sensors as a function of the thickness of the outer ZnO layer is shown in Figure 3a. The resistance increases with increasing the thickness of the ZnO layer up to 20 nm. A further increase in the ZnO thickness has the opposite effect on the resistance. As shown in Figure 3b, ZnO HFs show a much higher response to CO than TiO_2 HFs, which is likely to be associated with the intrinsic properties of ZnO and TiO_2 as semiconductors. The response to CO shows a bell-shaped curve as a function of the ZnO layer thickness, with a peak at 20 nm, in agreement with the trend shown by the resistance. In sharp contrast with the

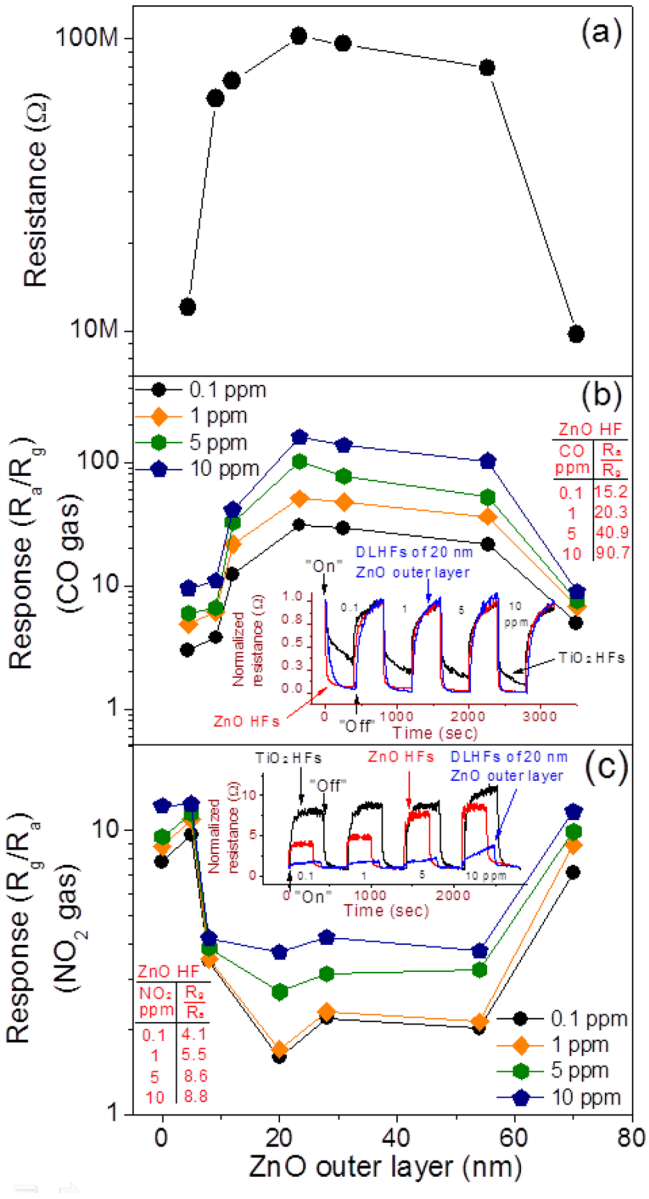

Figure 3. (a) Initial resistance of TiO_2/ZnO DLHFs as a function of the outer layer thickness, in air at 375 °C. Response of DLHFs to (b) CO and (c) NO_2 as a function of ZnO outer layer thickness. The insets in panels b and c are the normalized resistance curves of ZnO HFs, TiO_2 HFs, and TiO_2/ZnO DLHFs with 20 nm thick outer layer.

dx.doi.org/10.1021/am506499e | ACS Appl. Mater. Interfaces 2014, 6, 21494−21499

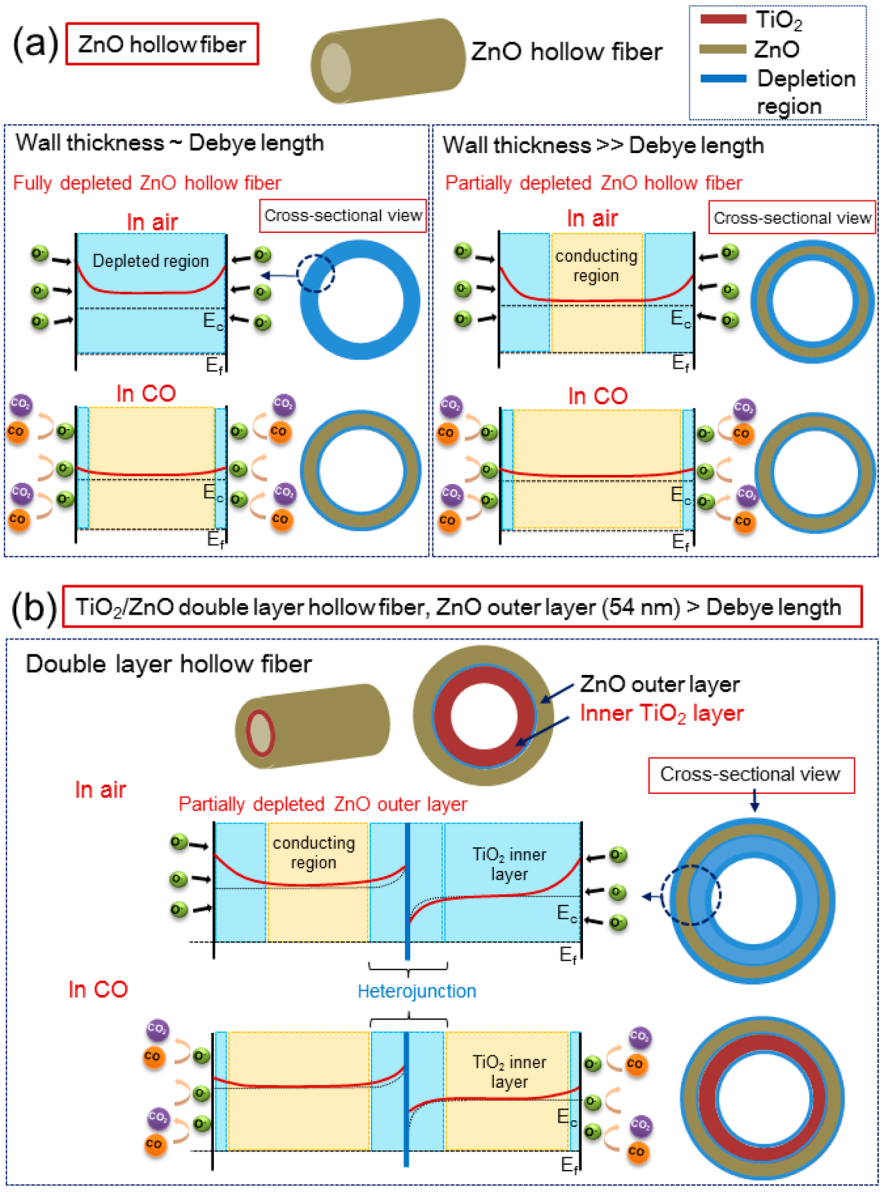

Figure 4. Schematic diagrams of sensing mechanism: (a) ZnO HFs with wall thickness $\sim\lambda_D$ and $\gg\lambda_D$, (b) TiO_2/ZnO DLHFs with outer layer thickness $>\lambda_D$ in the presence of CO gas. E_C and E_F indicate the conduction band minimum level and the Fermi energy level, respectively.

response to CO, the response to NO_2 of DLHFs with 20 nm thick ZnO layer is lower than the response observed in both TiO_2 and ZnO HFs, as shown in Figure 3c. DLHFs revealed improved CO-sensing properties compared to regular single-layer ZnO HFs for the same ZnO layer thickness. This is because single-layer ZnO HFs having a wall thickness thinner than or equal to λ_D are highly electron-depleted by adsorbed oxygen species when exposed to air, due to the ZnO tendency to capture electrons in its conduction band, therefore they are highly resistive. The width of the electron depletion layer is equal to λ_D of pure ZnO found in case of oxygen adsorption, and it is defined as[15]

$$\lambda_d = \left[\frac{2\varepsilon \mathrm{ZnO}\varphi}{q^2 N_{\mathrm{ZnO}}}\right]^{1/2} \quad (3)$$

where ϕ is the height of the potential barrier established by the oxygen adsorption,[16] ε_{ZnO} is the permittivity of ZnO, N_{ZnO} is the electron concentration in ZnO, and q is the charge of an electron, equivalent to 1.6×10^{-19} C. At room temperature, when $N_{ZnO} \sim 10^{18}$ cm^{-3},[16,17] $\varepsilon_{ZnO} \sim 8.7$,[18] and $\phi \sim 0.5$ eV,[19] the calculated λ_d is approximately 22 nm. In literature, the value of λ_D for bulk ZnO is in the range of 20−35 nm.[10,11] In this condition, when reducing gases such as CO are supplied to ZnO HFs, the adsorbed oxygen species will interact with the supplied reducing gas molecules, forming volatile species keen to evaporate and releasing the captured electrons back to the ZnO HFs. Following this process, the originally completely electron-depleted region will turn into a partially electron-depleted region, generating a sort of conduction channel and promoting a high change in resistance. Conversely, when ZnO HFs are thicker than λ_D, adsorbed oxygen from air will not make them completely electron-depleted, although they will induce a partially electron-depleted layer. The transition from the partial electron-depleted state to the complete electron-depleted state provides a lower resistance change during the cycle supply/cutoff of reducing gases. This explains why HFs

with a thinner fiber wall are better for the detection of reducing gases.

In the case of DLHFs, λ_D is the same because the outer surface, ZnO, is the same. At the interface between ZnO and TiO_2, electrons in the conduction band of ZnO flow to the conduction band of TiO_2,[20] because the work function of ZnO is lower than that of TiO_2, as shown in Figure S4 of the Supporting Information. The width of the space-charge region ($W_{heterojunction}$) can be calculated using eq 4[21]

$$W_{heterojunction} = \left[\frac{2\varepsilon_{ZnO}V_0}{q} \times \left\{\frac{N_{ZnO}}{N_{ZnO} \times (N_{TiO_2} + N_{ZnO})}\right\}\right]^{1/2} \quad (4)$$

where V_0, the contact potential difference between TiO_2 and ZnO, is 0.25 V, and N_{TiO_2} and N_{ZnO} are the electron concentrations, $\sim 10^{19}$ and $\sim 10^{18}$ cm^{-3}, respectively.[16,17,22] The calculated $W_{heterojunction}$ is ~4 nm. In addition, λ_d for the TiO_2 layer was found to be ~22 nm, as calculated by using eq 3, with $\varepsilon_{TiO_2} \sim 47.1$,[23] $q = 1.6 \times 10^{-19}$ C, $N_{TiO_2} \sim 10^{19}$ cm^{-3} at room temperature, and ϕ ~0.9 eV.[24] Consequently, a TiO_2 layer with a thickness of ~30 nm is likely to be completely electron depleted (see Figure S5 of the Supporting Information). It is worth noticing here that the space-charge layer is wider than λ_D, suggesting that, for the same layer thickness, the ZnO layer in DLHFs is more electron-depleted than the ZnO layer in HFs, as shown in Figure 4b. This is the reason why, in DLHFs, the exposure to reducing gases such as CO causes a higher resistance variation than in regular HFs, and why DLHFs revealed superior CO-sensing properties compared to single-layer HFs with the same fiber wall thickness. Conversely, gas response in DLHFs decreases for oxidizing gases such as NO_2. Because the outer layer is thinner than or equal to λ_D, it is completely electron-depleted in air; consequently, few electrons are available for incoming oxidizing gas molecules, leading to a lower resistance variation.

4. CONCLUSIONS

DLHFs were proven to be advantageous over regular single-layer HFs for the detection of reducing gases. Specifically, TiO_2/ZnO DLHFs were investigated as a representative system. By sequential deposition of TiO_2 and ZnO using ALD on polymeric fibers used as a sacrificial template and a subsequent thermal treatment, DLHFs were synthesized in a stable form. Their sensing properties under exposure to CO and NO_2 as representative of a reducing and an oxidizing gas, respectively, were investigated as a function of the thickness of the ZnO outer layer. DLHFs demonstrated a better behavior compared to HFs when detecting reducing gases such as CO, but showed a lower response to oxidizing gases such as NO_2. The inner TiO_2 layer is responsible for electron absorption, enabling to use a thicker outer layer than the one that would be required to achieve the same sensing properties in case of HFs. The use of DLHFs is a potentially novel approach to the fabrication of sensitive sensors for reducing gases based on oxide fibers.

■ ASSOCIATED CONTENT

Supporting Information

XRD patterns of TiO_2/ZnO DLHFs with different ZnO layer thicknesses, resistance curves of TiO_2 HFs and TiO_2/ZnO DLHFs and summarized gas responses of TiO_2/ZnO DLHFs in comparison to TiO_2 and ZnO HFs under exposure to CO, resistance curves of TiO_2 HFs and TiO_2/ZnO DLHFs and summarized gas responses of TiO_2/ZnO DLHFs in comparison to TiO_2 and ZnO HFs under exposure to NO_2, energy band structure of ZnO−TiO_2 heterojunction, and schematic diagrams of sensing mechanism in TiO_2/ZnO DLHFs based on radial variation of electron-depleted outer layer under exposure to CO gas. This material is available free of charge via the Internet at http://pubs.acs.org.

■ AUTHOR INFORMATION

Corresponding Author

*S. S. Kim. E-mail: sangsub@inha.ac.kr.

Author Contributions

S.S.K. conceived the study and prepared the paper. A.K. and J.-H.K. designed and performed the experiments. All authors have given approval to the final version of the paper.

Notes

The authors declare no competing financial interest.

■ ACKNOWLEDGMENTS

This work was supported by National Research Foundation of Korea (NRF) grant funded by the Ministry of Education, Science and Technology (MEST) of Korea (no. 2012R1A2A2A01013899) and the International Research & Development Program of NRF funded by MEST (no. 2013K1A3A1A21000149).

■ REFERENCES

(1) Zhang, Z.; Li, X.; Wang, C.; Wei, L.; Liu, Y.; Shao, C. ZnO Hollow Nanofibers: Fabrication from Facile Single Capillary Electrospinning and Applications in Gas Sensors. *J. Phys. Chem. C* **2009**, *113*, 19397−19403.

(2) Choi, S.-W.; Zhang, J.; Akash, K.; Kim, S. S. H_2S Sensing Performance of Electrospun CuO-Loaded SnO_2 Nanofibers. *Sens. Actuators, B* **2012**, *185*, 54−60.

(3) Choi, S.-W.; Katoch, A.; Zhang, J.; Kim, S. S. Electrospun Nanofibers of CuO-SnO_2 Nanocomposite as Semiconductor Gas Sensors for H_2S Detection. *Sens. Actuators, B* **2013**, *176*, 585−591.

(4) Katoch, A.; Sun, G.-J.; Choi, S.-W.; Byun, J.-H.; Kim, S. S. Competitive Influence of Grain Size and Crystallinity on Gas Sensing Performances of ZnO Nanofibers. *Sens. Actuators, B* **2013**, *185*, 411−416.

(5) Xu, L.; Zheng, R.; Liu, S.; Song, J.; Chen, J.; Dong, B.; Song, H. NiO@ZnO Heterostructured Nanotubes: Coelectrospinning Fabrication, Characterization, and Highly Enhanced Gas Sensing Properties. *Inorg. Chem.* **2012**, *51*, 7733−7740.

(6) Choi, K.-I.; Kim, H.-R.; Lee, J.-H. Enhanced CO Sensing Characteristics of Hierarchical and Hollow In_2O_3 Microspheres. *Sens. Actuators, B* **2009**, *138*, 497−503.

(7) Park, J. Y.; Choi, S.-W.; Kim, S. S. A Synthesis and Sensing Application of Hollow ZnO Nanofibers with Uniform Wall Thicknesses Grown Using Polymer Templates. *Nanotechnology* **2010**, *21*, 475601.

(8) Zhang, J.; Choi, S.-W.; Kim, S. S. Micro- and Nano-Scale Hollow TiO_2 Fibers by Coaxial Electrospinning: Preparation and Gas Sensing. *J. Solid State Chem.* **2011**, *184*, 3008−3013.

(9) Li, X.; Sun, P.; Yang, T.; Zhao, J.; Wang, Z.; Wang, W.; Liu, Y.; Lu, G.; Du, Y. Template-Free Microwave-Assisted Synthesis of ZnO Hollow Microspheres and Their Application in Gas Sensing. *CrystEngComm* **2013**, *15*, 2949−2955.

(10) Look, D. C. Recent Advances in ZnO Materials and Devices. *Mater. Sci. Eng., B* **2001**, *80*, 383−387.

(11) Jin, C.; Park, S.; Kim, H.; Lee, C. Ultrasensitive Multiple Networked Ga_2O_3-Core/ZnO-Shell Nanorod Gas Sensors. *Sens. Actuators, B* **2012**, *161*, 223−228.
(12) Choi, S.-W.; Park, J. Y.; Lee, C.; Lee, J. G.; Kim, S. S. Synthesis of Highly Crystalline Hollow TiO_2 Fibers Using Atomic Layer Deposition on Polymer Templates. *J. Am. Ceram. Soc.* **2011**, *94*, 1974−1977.
(13) Katoch, A.; Choi, S.-W.; Kim, S. S. Effect of the Wall Thickness on the Gas-Sensing Properties of ZnO Hollow Fibers. *Nanotechnology* **2014**, *25*, 455504.
(14) Katoch, A.; Choi, S.-W.; Sun, G.-J.; Kim, S. S. Pt Nanoparticle-Decorated ZnO Nanowire Sensors for Detecting Benzene at Room Temperature. *J. Nanosci. Nanotechnol.* **2013**, *13*, 7097−7099.
(15) Vanheusden, K.; Warren, W. L.; Seager, C. H.; Tallant, D. R.; Voigt, J. A.; Gnade, B. E. Mechanisms behind Green Photoluminescence in ZnO Phosphor Powders. *J. Appl. Phys.* **1996**, *79*, 7983−7990.
(16) Maragliano, C.; Lilliu, S.; Dahlem, M. S.; Chiesa1, M.; Souier, T.; Stefancich, M. Quantifying Charge Carrier Concentration in ZnO Thin Films by Scanning Kelvin Probe Microscopy. *Sci. Rep.* **2014**, *4*, 4203.
(17) Ellmer, K. *Transparent Conductive Zinc Oxide*, Springer Series in Materials Science; Springer: Berlin/Heidelberg, 2008.
(18) Look, D. C.; Hemsky, J. W. Residual Native Shallow Donor in ZnO. *Phys. Rev. Lett.* **1999**, *82*, 2552−2555.
(19) Liao, Z.-M.; Liu, K.-J.; Zhang, J.-M.; Xu, J.; Yu, D.-P. Effect of Surface States on Electron Transport in Individual ZnO Nanowires. *Phys. Lett. A* **2007**, *367*, 207−210.
(20) Kayaci, F.; Vempati, S.; Ozgit-Akgun, C.; Donmez, I.; Biyikliab, N.; Uyar, T. Selective Isolation of the Electron or Hole in Photocatalysis: ZnO−TiO_2 and TiO_2−ZnO Core−Shell Structured Heterojunction Nanofibers via Electrospinning and Atomic Layer Deposition. *Nanoscale* **2014**, *6*, 5735−5745.
(21) Streetman, B. G.; Banerjee, S. K. *Solid State Electronic Devices*, 6th ed.; Pearson Education Inc.: Upper Sadde River, NJ, 2005.
(22) Seger, B.; Tilley, S. D.; Pedersen, T.; Vesborg, P. C. K.; Hansen, O.; Grätzel, M.; Chorkendor, I. Silicon Protected with Atomic Layer Deposited TiO_2: Conducting versus Tunnelling through TiO_2. *J. Mater. Chem. A* **2013**, *1*, 15089−15094.
(23) Wei, D.; Hossain, T.; Garces, N. Y.; Nepal, N.; Meyer, H. M.; Kirkham, M. J.; Eddy, C. R., Jr; Edgara, J. H. Influence of Atomic Layer Deposition Temperatures on TiO_2/n-Si MOS Capacitor. *J. Solid State Sci. Technol.* **2013**, *2*, N110−N114.
(24) Mondal, A.; Dhar, J. C.; Chinnamuthu, P.; Singh, N. K.; Chattopadhyay, K. K.; Das, S. K.; Das, S. C.; Bhattacharyya, A. Electrical Properties of Vertically Oriented TiO_2 Nanowire Arrays Synthesized by Glancing Angle Deposition Technique. *Electron. Mater. Lett.* **2013**, *9*, 213−217.